Journal of Geophysical Research: Solid Earth

Supporting Information for

Temperature, lithosphere–asthenosphere boundary, and heat flux beneath the Antarctic Plate inferred from seismic velocities

Meijian An[1,*], Douglas A. Wiens[2], Yue Zhao[1], Mei Feng[1], Andrew Nyblade[3], Masaki Kanao[4], Yuansheng Li[5], Alessia Maggi[6], Jean-Jacques Lévêque[6]

1, Institute of Geomechanics, Chinese Academy of Geological Sciences, Beijing, China

2, Dept of Earth and Planetary Sci, Washington University, St. Louis, MO, USA

3, Dept of Geosciences, Penn State University, University Park, PA, USA

4, National Institute of Polar Research, Tokyo, Japan

5, Polar Research Institute in China, Shanghai, China

6, Institut de Physique du Globe de Strasbourg, Université de Strasbourg/EOST, CNRS, Strasbourg, France

Contents of this file

Figures S1 to S10
References

Introduction

This file includes ten supporting figures, Figures S1–S10, as below.

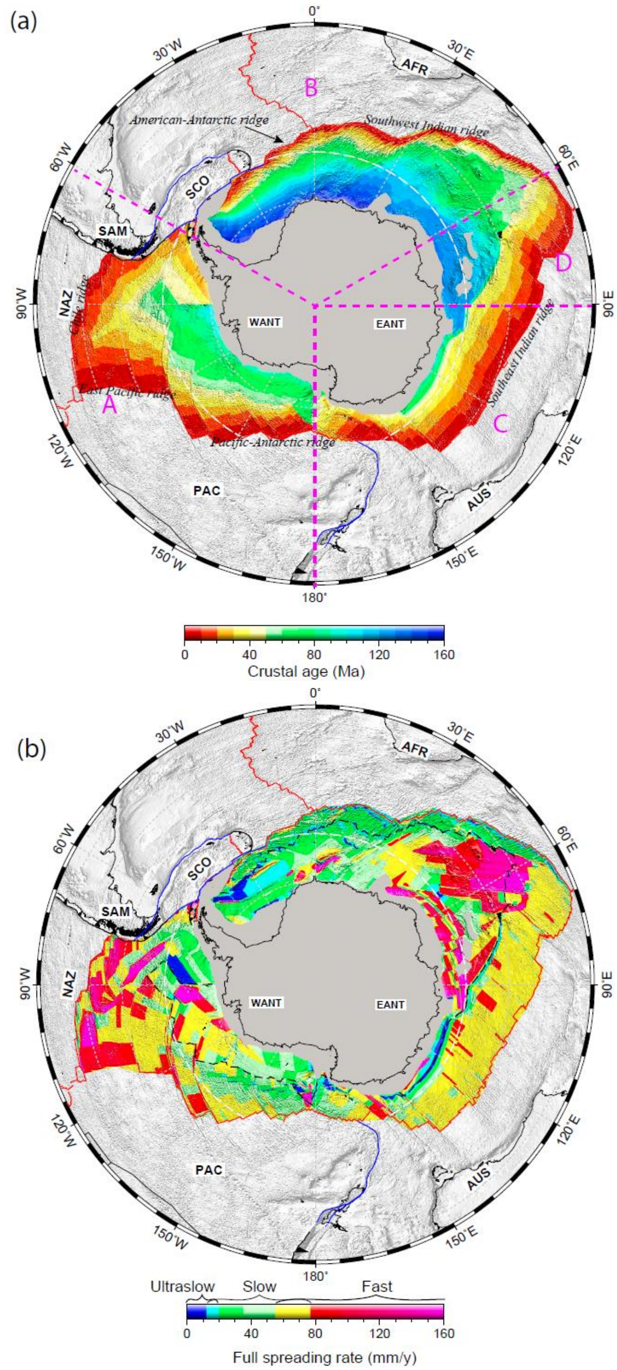

(a)
0°
30°W
30°E
AFR
B
American-Antarctic ridge
Southwest Indian ridge
60°W
60°E
SCO
SAM
D
90°W
90°E
NAZ
WANT
EANT
East Pacific ridge
Southeast Indian ridge
A
C
Pacific-Antarctic ridge
120°W
120°E
PAC
AUS
150°W
150°E
180°
0 40 80 120 160
Crustal age (Ma)
(b)
Ultraslow
Slow
Fast
0 40 80 120 160
Full spreading rate (mm/y)

Figure S1. Oceanic floor (a) age and (b) full spreading rate for the Antarctic Plate. Data are from *Müller et al.* [2008]. Spreading-rate classifications of 'ultraslow' and 'slow' are defined according to *Dick et al.* [2003]. The dashes in (a) mark a crustal age contour of 55 Ma. Most of the oceanic lithosphere beneath the Antarctic plate was formed at slow-spreading ridges (<77 mm/yr); ultra-slow spreading has occurred along the African–Antarctic (or Southwest Indian) and American–Antarctic ridges (<20 mm/yr). The oceanic crust west of the Antarctic Peninsula is young.

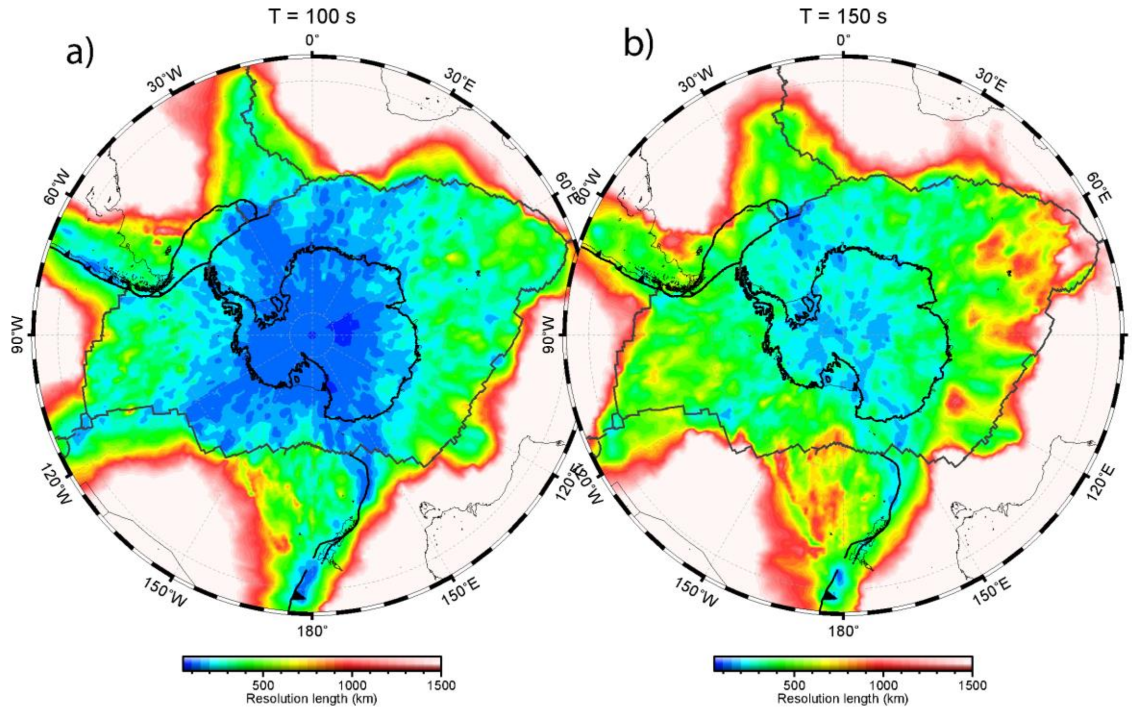

Figure S2. Resolution length distribution for Rayleigh-wave dispersions at periods of (a) 100 s and (b) 150 s. All maps are from *An et al.* [2015], and topographic data are from ETOPO2.

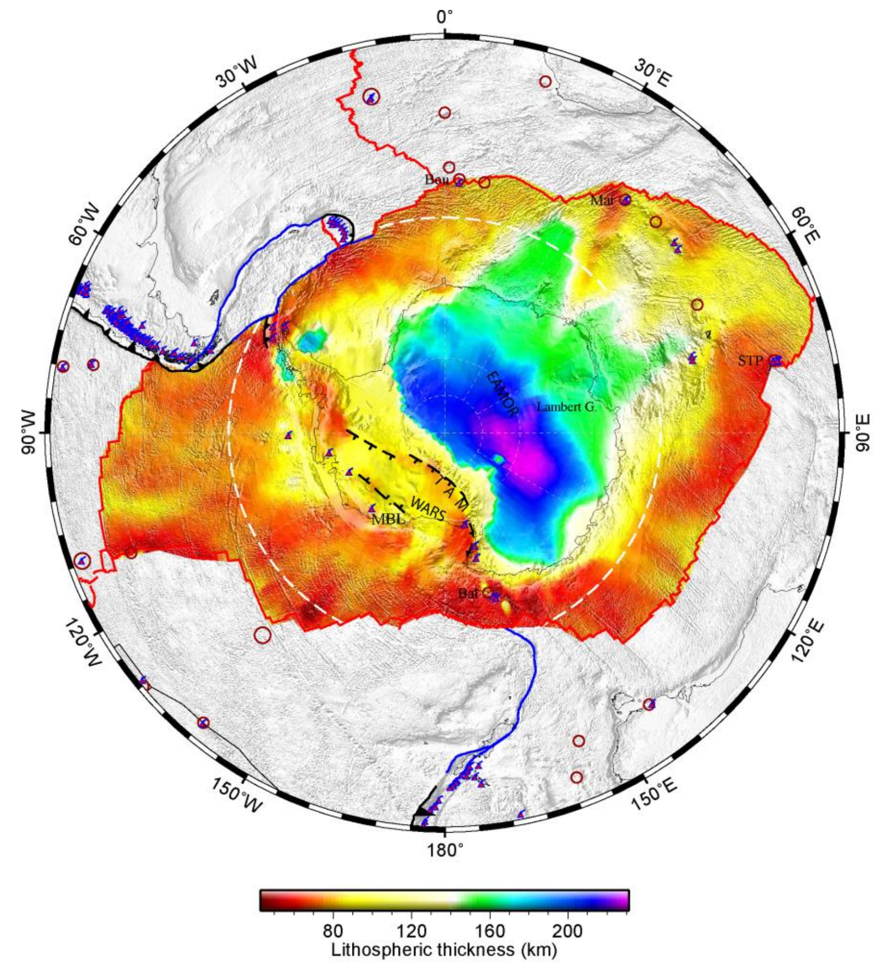

Figure S3. Topographic map of the lithosphere base of the Antarctic Plate, also showing the locations of volcanoes and hotspots. The LAB map is the same as in Figure 6. Other symbols are as in Figure 1.

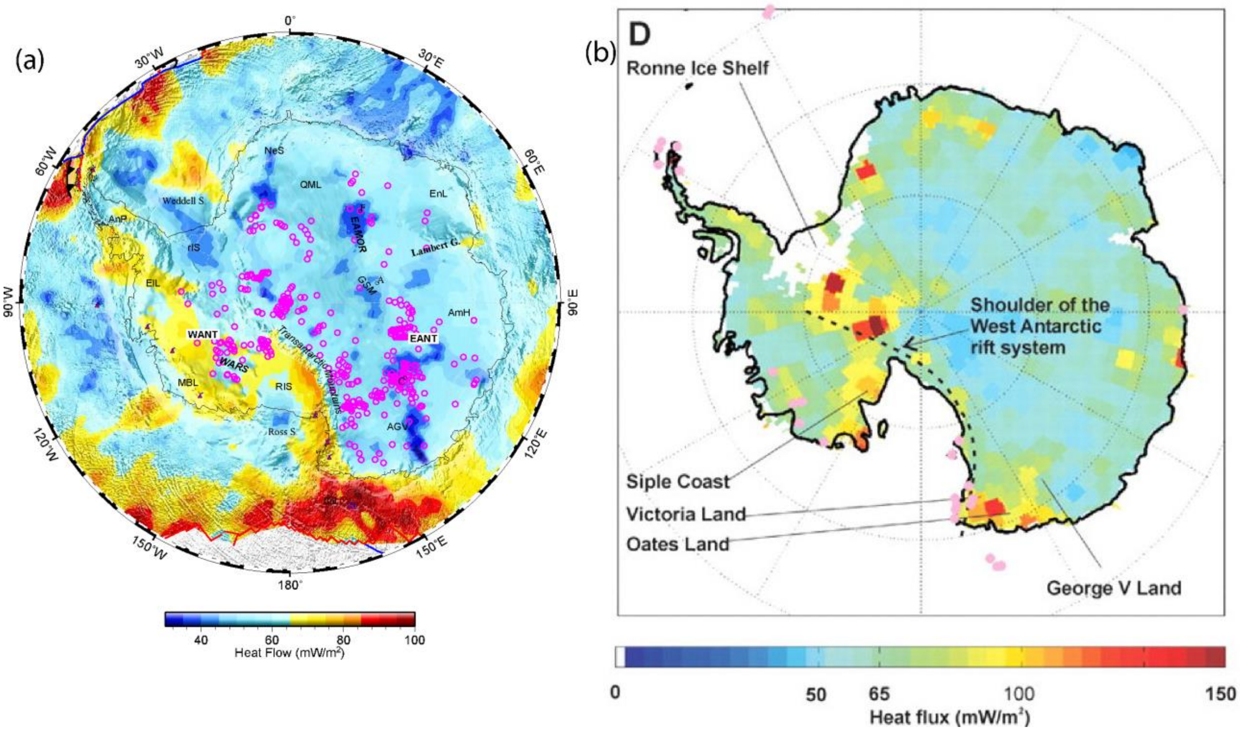

Figure S4. (a) Heat flow and subglacial lakes (open purple circles) in Antarctica. Heat fluxes are the same as in Figure 8, and the subglacial lake data are from *Wright and Siegert* [2012]. (b) Reproduction of fig. 1D (Heat flow in Antarctica) from *Maule et al.* [2005] for comparison.

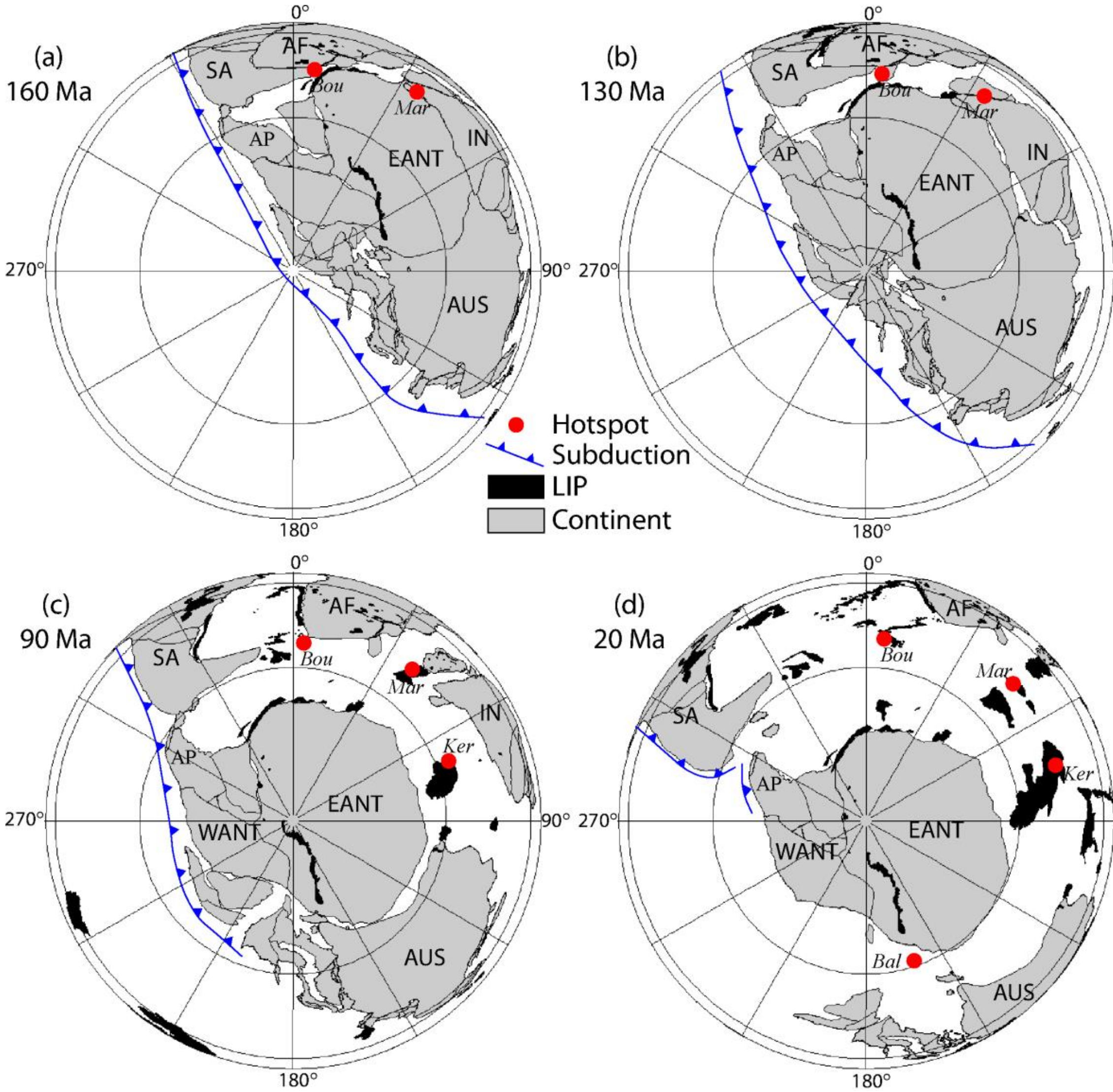

Figure S5. Tectonic evolution of Gondwana during the past 160 Myr (see also fig. S3 in *An et al.* [2015]). AF = African continent; AP = Antarctic Peninsula; AUS = Australian continent; Bal = Balleny hotspot; Bou = Bouvet hotspot; EANT = East Antarctica; IN = Indian continent; Ker = Kerguelen hotspot; LIP = Large Igneous Province; Mar = Marion hotspot; SA = South American continent. Continental reconstructions and the locations of large igneous provinces are from *Schettino and Scotese* [2005]. Subduction zones shown in panels (a–c) are adapted from *Torsvik et al.* [2008], and in (d) are from *Breitsprecher and Thorkelson* [2009]. The locations of the Bouvet, Kerguelen, and Marion hotspots are from *Torsvik et al.* [2008].

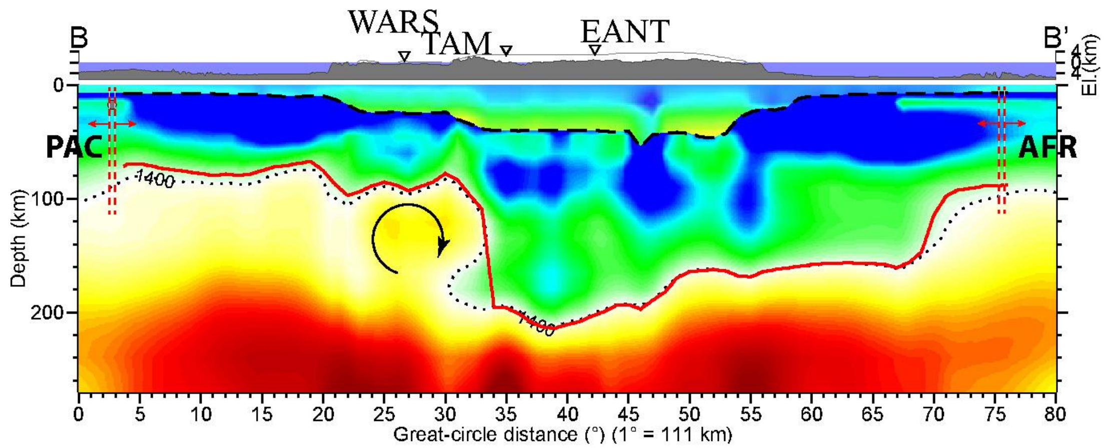

Figure S6. Illustration of a small, sub-lithospheric scale convection cell (circle with arrow) beneath the West Antarctic rift system. The image and symbols are the same as in Figure 5b.

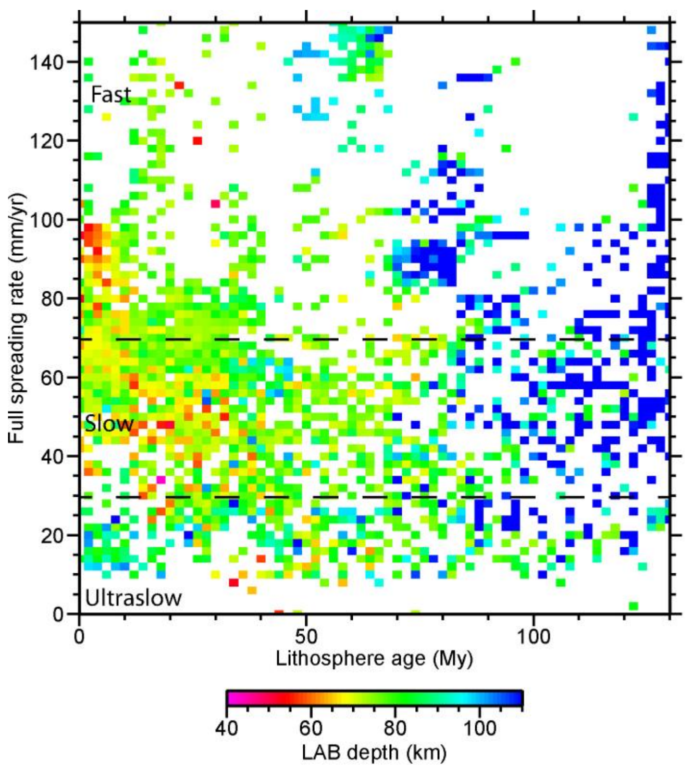

Figure S7. LAB depths as a function of crustal age and spreading rate. Crustal ages and spreading rates are the same as those in Figure S1. Two dashed lines separate three regions generally corresponding to ultraslow, slow, and fast spreading rates. The definition on the rates in this figure differs little from that (see Fig. S1b) in *Dick et al.* [2003].

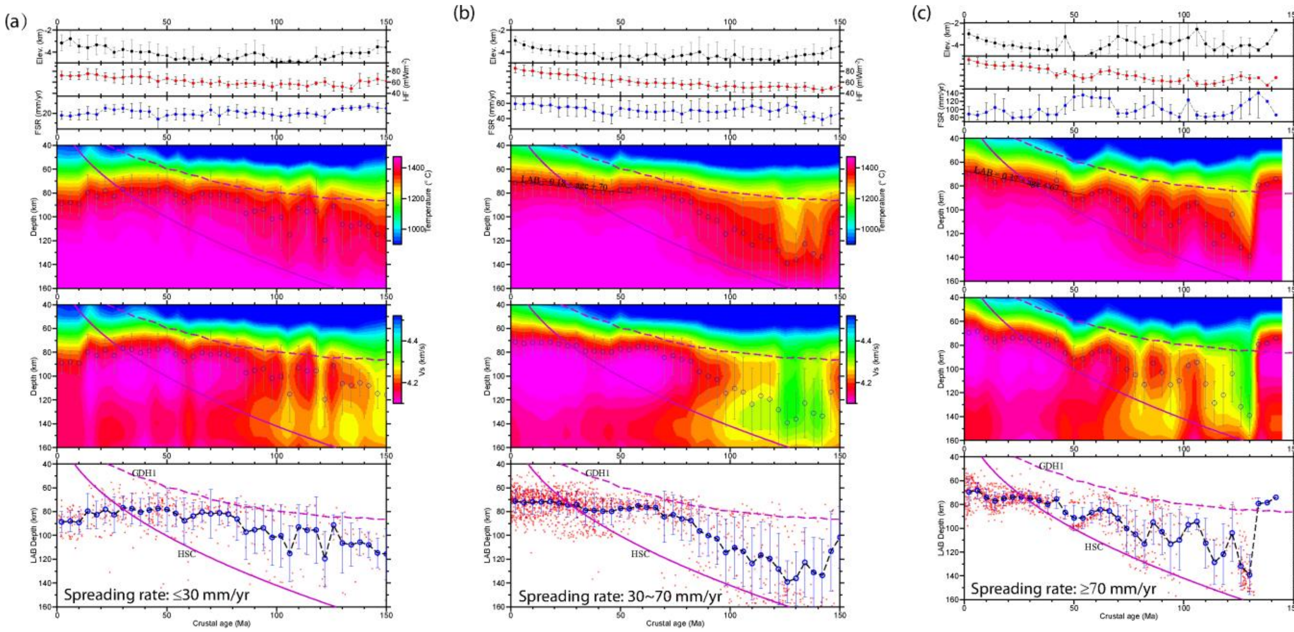

Figure S8. In each column, from top to bottom: average oceanic seafloor elevation, heat flux (HF), full spreading rate (FSR), deep temperature/*S* velocity, and LAB depth as a function of crustal age for ocean crust created at (a) ultraslow (<30 mm/yr; see Fig. 11b)), (b) slow (30–70 mm/yr) and (c) fast (>70 mm/yr) spreading ridges. The ranges of spreading rates are the same as those in Figure S7. Red circles represent the information of an equal-area cell in the oceanic region, and blue circles are their means in 4-Myr bins with error bars of one standard deviation. Crustal age and rate data are the same as in Figure S1, and lithospheric thicknesses are from Figure 6. Purple dashes represent the LAB determined from the temperatures predicted by the GDH1 model, and the purple line is from the temperatures predicted by the half-space cooling model (HSC). LAB definition for the curves is the same as for Figure 6, but different from *Stein and Stein* [1992]. The black line in (b,c) was obtained by linear regression of the relationship between thickness and crustal age for ages of ≤55 Ma.

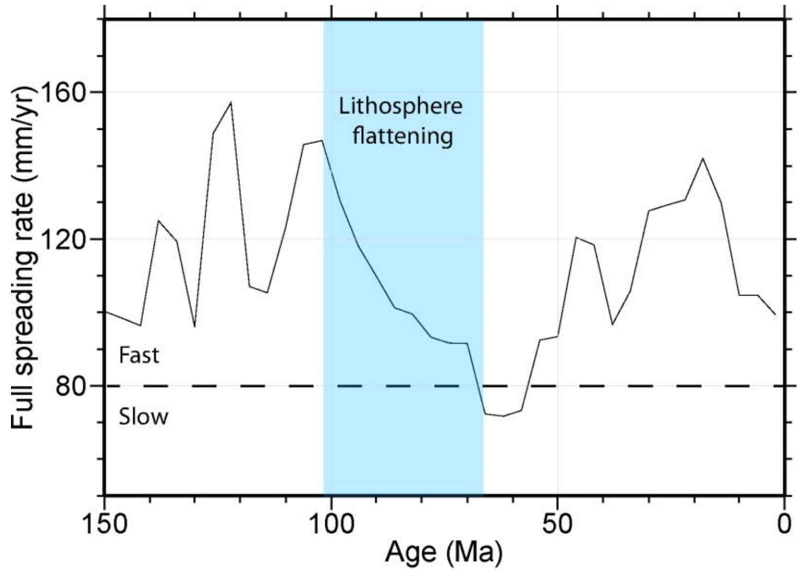

Figure S9. Full spreading rate as a function of oceanic crust age for the Pacific Plate. Data are the same as in Figure S1. Iso-velocity contours of the lithospheric upper mantle of the Pacific Plate flatten at ages of 70–100 Ma. The lithosphere with flat iso-velocity contours was created when the spreading rate gradually decreased (shaded area) from fast (146 mm/yr at 102 Ma) to slow (<80 mm/yr at 65 Ma) over a ~40 Myr period. The spreading rate variation over this period (~65–102 Ma) is distinct from that at other times, suggesting that flattening of the Pacific Plate was related to the spreading rate of the ridge where the lithosphere was created, even though this relationship is poorly understood.

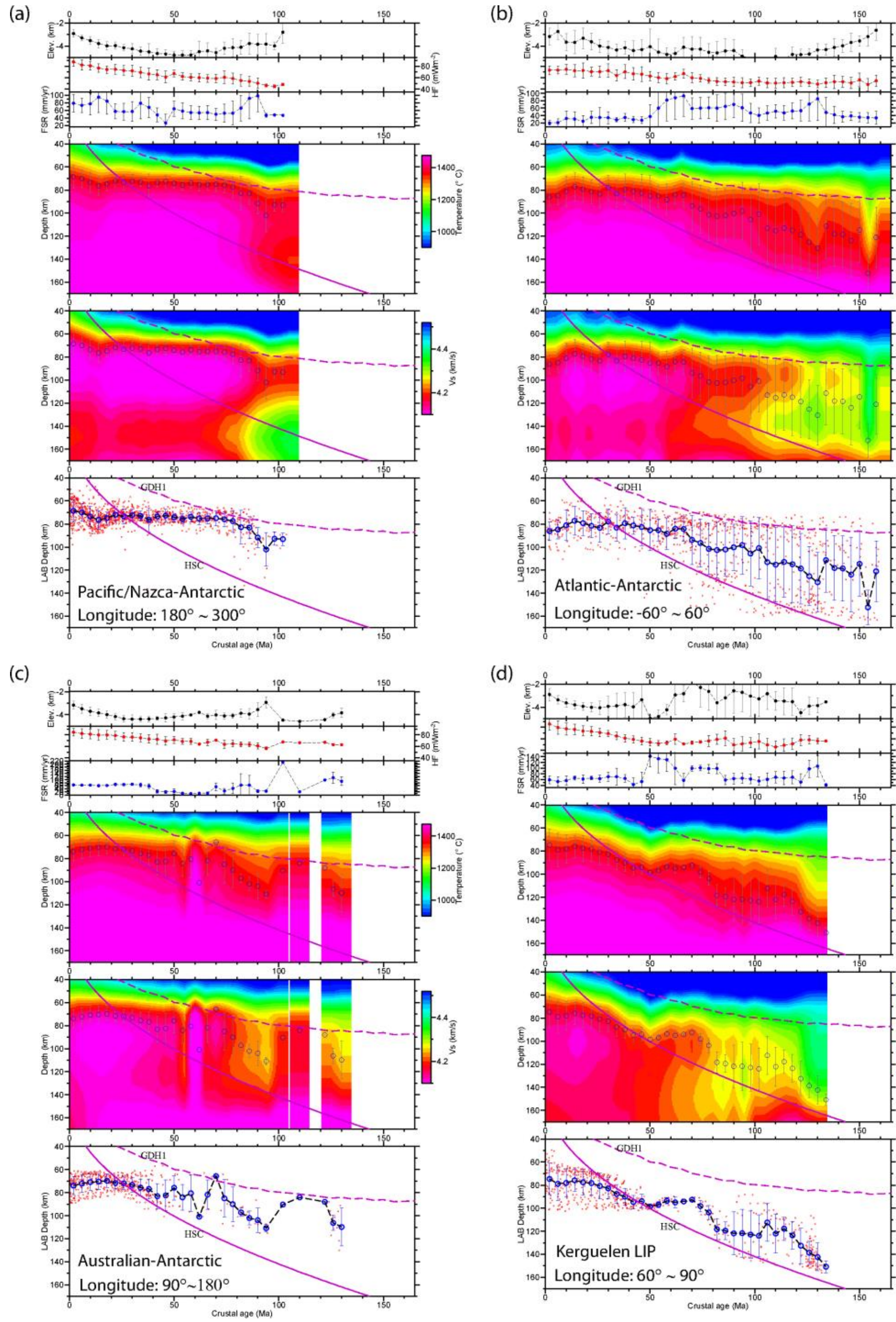

Figure S10. In each column, from top to bottom: average oceanic seafloor elevation, heat flux (HF), full spreading rate (FSR), deep temperature/*S* velocity, and LAB depth as a function of crustal age for oceanic crust created at the (a) Pacific/Nazca–Antarctic ridge, (b) Atlantic–Antarctic ridge, (c) Australian–Antarctic ridge, and oceanic crust (d) close to the Kerguelen Plateau. The region of each subfigure is indicated in Figure S1a by purple dashes. Other symbols are as in Figure S8. For young lithosphere, oceanic floor subsides with increasing age, and LAB depth increases, as expected. A large fluctuation in the age–thickness relationship is observed in the Kerguelen Large Igneous Province (d). This province was produced by a hotspot at ~118 Ma [*Anderson*, 2005], and the present-day volcanoes in (d) are close to the St. Paul–Amsterdam hotspot that is still active. Similarly, the distinctive variations in (a–c) may be attributed to regional tectono-thermal effects.

References

An, M., D. A. Wiens, Y. Zhao, M. Feng, A. A. Nyblade, M. Kanao, Y. Li, A. Maggi, and J. Lévêque (2015), S-velocity model and inferred Moho topography beneath the Antarctic Plate from Rayleigh waves, *J. Geophys. Res.*, 120, 359-383, doi:10.1002/2014JB011332.

Anderson, D. L. (2005), Scoring hotspots: The plume and plate paradigms, *Geological Society of America Special Papers*, 388, 31-54, doi:10.1130/0-8137-2388-4.31.

Breitsprecher, K., and D. J. Thorkelson (2009), Neogene kinematic history of Nazca–Antarctic – Phoenix slab windows beneath Patagonia and the Antarctic Peninsula, *Tectonophysics*, 464, 10-20, doi:10.1016/j.tecto.2008.02.013.

Dick, H. J. B., J. Lin, and H. Schouten (2003), An ultraslow-spreading class of ocean ridge, *Nature*, 426, 405-412.

Müller, R. D., M. Sdrolias, C. Gaina, and W. R. Roest (2008), Age, spreading rates, and spreading asymmetry of the world's ocean crust, *Geochem. Geophys. Geosyst.*, 9, Q04006, doi:10.1029/2007gc001743.

Maule, C. F., M. E. Purucker, N. Olsen, and K. Mosegaard (2005), Heat flux anomalies in Antarctica revealed by satellite magnetic data, *Science*, 309, 464-467, doi:10.1126/science.1106888.

Schettino, A., and C. R. Scotese (2005), Apparent polar wander paths for the major continents (200 Ma to the present day): a palaeomagnetic reference frame for global plate tectonic reconstructions, *Geophys. J. Int.*, 163, 727-759, doi:10.1111/j.1365-246X.2005.02638.x.

Stein, C. A., and S. Stein (1992), A model for the global variation in oceanic depth and heat flow with lithospheric age, *Nature*, 359, 123-129.

Torsvik, T. H., C. Gaina, and T. F. Redfield (2008), Antarctica and Global Paleogeography: From Rodinia, Through Gondwanaland and Pangea, to the Birth of the Southern Ocean and the Opening of Gateways, in Antarctica: A Keystone in a Changing World —Online Proceedings of the 10th International Symposium on Antarctic Earth Sciences., edited by A. K. Cooper, et al., p. kp11, The National Academies Press, Washington, DC.

Wright, A., and M. Siegert (2012), A fourth inventory of Antarctic subglacial lakes, Antarct. Sci., 24, 659-664, doi:10.1017/S095410201200048X.